IOP Conf. Series: Materials Science and Engineering **406** (2018) 012041 doi:10.1088/1757-899X/406/1/012041

Flexural behavior and damage extent in woven natural fibers/polypropylene composite laminates

Pietro Russo[1], Giorgio Simeoli[1], Vito Pagliarulo[2], Vittorio Bianco[1,2], Pietro Ferraro[2]

[1] Institute for Polymers, Composites and Biomaterials, National Council of Research, Pozzuoli (Na), Italy
[2] Institute of Applied Sciences and Intelligent Systems, National Council of Research, Pozzuoli (Na), Italy

Abstract. Recently, low environmental impact and potential use in a wide range of applications have been the main driving reasons supporting the rapid growth of the research interest toward the investigation and development of items based on natural fiber composites. This paper compares the performance and the extent of damage suffered by polypropylene (PP) composites reinforced with natural fiber fabrics and subjected to flexural loads. In particular, laminates including jute, flax and basalt woven fibers have been prepared by typical film stacking and compression molding techniques. A premodified matrix (PPC) including 2 wt% of a coupling agent was also considered. Measurements were carried out on at least 5 determinations for each kind of samples. All flexural parameters appeared to be significantly increased for specimens based on PPC with respect to the ones based on neat PP with effects particularly pronounced in presence of basalt fibers. Despite the use of the same content of coupling agent, this finding can be attributed the achievement of a different extent of interfacial adhesion, in turn, due to the different nature of reinforcing fibers. The influence of both the matrix modification and the nature of reinforcing fibers on the extent of induced flexural damage were assessed in non-destructive way by Electronic Speckle Pattern Interferometry and by Scanning Electron Microscopy observations of cryofractured surfaces.

1. Introduction

In the last years, the increased sensibleness about environmental concerns and depletion of fossil sources have stimulated a growing interest toward new-ecosustainable materials as the natural fiber composites (NFC). In fact, the advantages derive also in that natural fibers are cheap, have low density and may offer specific properties higher (eg. linen fibers) or, at least, superior to those of other synthetic ones conventionally used for reinforcements (i.e. glass, carbon fibers). On the other side, drawbacks as incompatibilities with the hosting matrices, their high sensitivity to processing conditions and the significant tendency to absorb moisture still reduce their potential applications. Therefore, special care must be devoted to improve the interfacial fiber-matrix adhesion through surface modification of the reinforcing fibers and/or with the aid of appropriate coupling agent to optimize the processing conditions and last an in-depth characterization is required with the aim to verify the meeting of suitable technical specifications [1]. Among these latter, a common requirement is the capability of the new material to support loads without failure for safety reasons.

For this purpose, the use of non-destructive testing techniques as ultrasonic methods [2], acoustic methods [3] and infrared thermography [4], that can be applied both remotely and in-line to monitor the behavior of reference materials during their loading, is increasingly common. In this frame, speckle interferometry is customary tool for precise measurements in engineering, displacement measurement, vibration analysis, velocity measurement, non-destructive testing [5-8] and it can be used on very different materials. In this paper, we have used the Electronic Speckle Pattern Interferometry (ESPI) as a tool to characterize in non-destructive way and at full field novel ecosustainable composite materials.

In particular, six different types of thermoplastic composite laminates were considered. All samples, including woven natural fibers were prepared by conventional film stacking and compression molding technologies. Tested specimens were investigated by ESPI to assess the effect of the main constituents 'nature on the detected extent of the damaged area. Moreover, results were also discussed in terms of morphological aspects by analyzing scanning electron microscopic observations of cryo-fractured surfaces taken in correspondence of the applied flexural load.

2. Experimental

2.1 Materials and sample preparation

Six different composite systems involving 4 matrices and three natural fiber fabrics were investigated. In details, samples were prepared from a polypropylene (PP) resin (Hyosung Topilene PP J640, MFI@230 °C, 2.16 kg: 10 g/10 min), also premixed with 2 wt% of a compatibilizing agent (PP-g-MA - Polybond 3000, MFI@190 °C, 2.16 kg: 405 g/10 min) (code PPC), a poly(lactic acid) (PLA – Ingeo 7001 D, ρ=1.24 g/cc, MFI@210 °C, 2.16 kg: 6 g/10 min, Tg=55-60 °C) and a polyamide 6 (PA6) (Lanxess Durethan B30S-000000 (MFI@260 °C, 5 kg: 102 g/10 min).

Films of all these matrices, obtained in pre-optimized conditions, were alternatively stacked with commercial reinforcing fiber fabrics. In particular, polypropylene, neat or modified, systems included a jute plain wave type fabric (J) with a specific mass of 250 g/m^2 by Deyute (Alicante, Spain), to make samples coded as PPJ and PPCJ, respectively, or a 2x2 twill flax fabric (L) supplied by Biotex (weight: 200 g/m^2), to prepare samples coded as PPL and PPCL, respectively. The PLA samples were reinforced with the above cited Jute fabric (PLAJ sample) while the polyamide 6 was reinforced by using a basalt plain wave type fabric (BS - weight: 210 g/m^2) from Incotelogy GmbH (Germany) (PA6BS).

Stacks of plastic films and reinforcing fabrics, made up of different number of layers, preliminarily estimated on the basis of the weight of the considered fabric and of previous experiences, to obtain laminates with thickness approximately equal to 3 mm, were compacted by a hot pressing step carried out under adequate temperature and pressure profile conditions.

2.2 Characterization techniques

Plates with dimensions of 100 mm × 12.7 mm were cut from the laminates and used for three-point bending tests on a Universal Testing Machine (Instron model 4505). Measurements were performed according to ASTM-D790 at a crosshead speed of testing equal to 2.47 mm/min, using a load cell of 1 kN and a span set at 70 mm at room temperature after being equilibrated under standard ASTM condition of 23 °C and 50% relative humidity for 24. Results are reported in terms of typical stress-strain curves and flexural parameters averaged on at least 5 determinations for each investigated sample.

A typical scheme of the system for recording speckle interferometric measurements can be found in [6]. The laser beam is split into a reference beam and an object beam by means of a Beam Splitter (BS). The reference beam is coupled into an optical fiber to reach a Charge-Coupled Device sensor (CCD), where also the light scattered from the object is addressed. Before reaching the object, the illumination beam passes through an electronically tilted etalon to shift the probing beam laterally in a parallel direction. In this way, it is possible to obtain multiple equivalent images of the speckle pattern, which are used to perform an average to reduce the speckle noise. Upon an external perturbation (i.e. thermal or mechanical), the plate is deformed and the reflected wavefront is slightly changed, while reference beam remains unperturbed. Thus,

the CCD camera records a new speckle pattern and the subtraction of the registered speckle patterns (deformed and non-deformed states) provides the correlation fringes. Analytically, the speckle pattern intensity for the unperturbed state is given by:

$$\boldsymbol{I_1 = I_0 + I_r + 2\sqrt{I_0 I_r}\,cos(\theta)}$$

while for the deformed state is given by:

$$\boldsymbol{I_1 = I_0 + I_r + 2\sqrt{I_0 I_r}\,cos(\theta + \phi)}$$

where I_0 is the intensity scattered from the object, I_r is the reference beam, θ is the phase angle and ϕ is related to the displacement, i.e. the deformation. The fringes pattern that represents the out-of-plane surface displacement is represented by the equation:

$$\boldsymbol{I_{1-2} = 2\sqrt{I_0 I_r}[cos\,\theta - cos(\theta + \phi)]}$$

The correlation fringes, digitally acquired and treated for contrast enhancement and noise removal, allow obtaining the phase contrast maps, from which it is possible to measure the displacement field with high accuracy [5].

3. Results and discussion

Results of static flexural tests are summarized by the histograms depicted in Figure 1a, b and c, in terms of flexural modulus, flexural strength and strain at the maximum load, respectively.

The data demonstrate an evident improvement in the flexural performances in presence of the compatibilizing agent for polypropylene composite laminates, as a sign of a superior adhesion at the fiber-matrix interface and, consequently, of the enhancement of stress transfer between the polymeric and the reinforcing phases. Expectedly, this behavior occurs at the expense of the strain at maximum load which, in both cases, is reduced with a more pronounced effect detected for composite specimens containing woven jute fibers.

The latter, also used for the PLA, give rise to fully biodegradable PLAJ systems with further increased flexural modulus but which show a flexural strength slightly lower than that obtained for the more resistant polypropylene sample (PPCL).

Finally, the chemical affinity between the polar polyamide 6 and the basalt fibers as well as the superior mechanical properties of basic constituents with respect to other matrices and reinforcing natural fibers herein considered justify the extraordinary performances of the PA6BS composite laminate.

a)

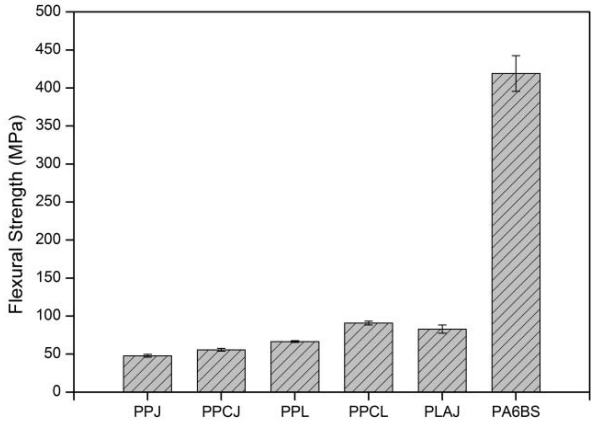

b)

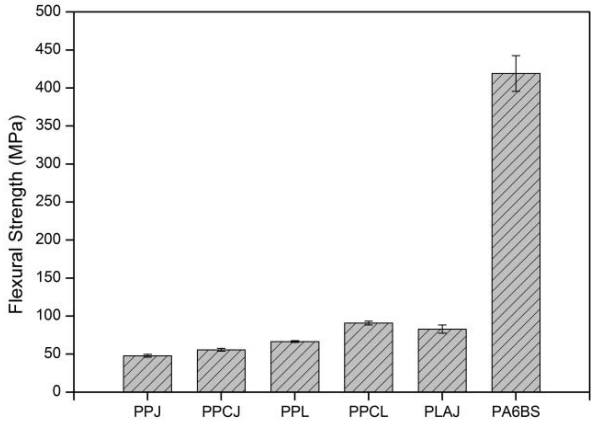

c)

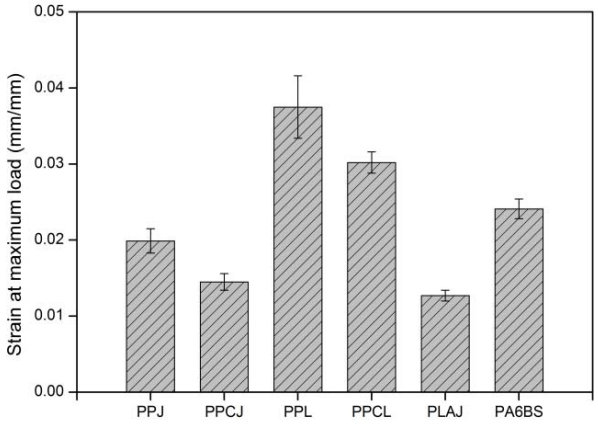

Figure 1. Flexural parameters of investigated composite systems

Figure 2 shows the process of estimation of the damaged area from the acquired fringe pattern in the specific case of the front side of a PA6BS specimen. In particular, the noisy phase map is reported in Figure 2(a). In order to obtain a reliable estimate of the damaged area, speckles need to be removed from the noisy map, which is achieved by means of an effective signal sparsity enhancement filter [9, 10]. The denoised map is shown in Figure 2(b), from which the central area of interest is selected (as shown in Figure 2(c)). Remarkably, numerical calibration is automatically performed in order to compensate for unwanted phase tilts eventually due to a non-perfect positioning of the specimen on the recording support. In this case, a second order polynomial fit was used. Hence, after calibration the estimated out-of-plane displacement is only due to the damage itself, i.e. the estimated value of the damaged area does not depend on the recording system. Figure 2(d) shows the area of interest after calibration, while the binary map in Figure 2(e) is obtained from (d) after applying image segmentation operators. This binary map is then used to measure the extent of the damaged area.

In this work, both sides of all the bended specimens were deformed by an external heating perturbation, focusing the attention on the section at which the flexural load was applied. Results showed that the damaged area is always higher on the back (tensile side) of the specimens with respect to the side where the force was applied (compression side). An exception is really the PA6/basalt system for which the extent of the damaged area evaluated on the front side seems to be even four times higher than the one recorded on the rear side. This behavior reflects the relatively high flexural rigidity of this system that induces a prevailing fiber breaking with respect to delamination phenomena on the tensile side of specimens and pronounced out-of-plane deformations on the loaded (front) side because of the hidden damages.

ESPI is able to assess the effective damaged area as well as the delaminated one by the measure of the specimen out-of-plane deformation due to a thermal stress and Figure 3 shows the extent of the damaged area for all investigated specimens. In this regard, it should be noted that inspections were carried out on specimens that have undergone a flexural deformation equal to 5%, as established by the reference ASTM Standard. In this cases, the value is always higher than that corresponding to the maximum load at which the incipient damage of included fibers is assumed. Therefore, the ESPI technique was used to compare the extent of the damaged area, due to the occurrence of various phenomena as delamination, fibers debonding, matrix cracking, fiber breaking and so on, for the different specimens, under the same flexural strain.

Clearly, the presence of the coupling agent in polypropylene composite laminates reinforced with jute fiber fabric, promoting a premature breaking of the reinforcing fibers, limits the delamination phenomena especially on the compression (front) side of the loaded specimen but the improved adhesion is not enough to prevent a certain sliding between adjacent plies on the back side, where the damage effects are particularly enhanced by tensile stresses. In this case, even because of the relatively low tensile properties of jute fibers in comparison with the other natural fibers considered in this research, the extent of the damaged area results to be comparable to that generated in presence of pure PP.

About composite samples including linen fibers, no damage seems to be verified on the front side, regardless the presence of the coupling agent. On the contrary, the damaged area on the tensile side is strongly affected by the improved interfacial adhesion: behavior reflecting the already mentioned effect of the PP-g-MA, more pronounced with respect to linen fibers with respect to jute fibers.

PLA/woven jute fibers specimens show damaged areas with significant extent only on the opposite side of the specimen with respect to the one where the load is applied.

Finally, the intrinsic good interfacial adhesion in PA6 systems including basalt fibers is responsible for the remarkable damage extent detected on both sides of the loaded specimens. However, surprisingly, it seems that the extent of the damage is wider on the side where the flexural load is applied. This unexpected consideration is still under investigation.

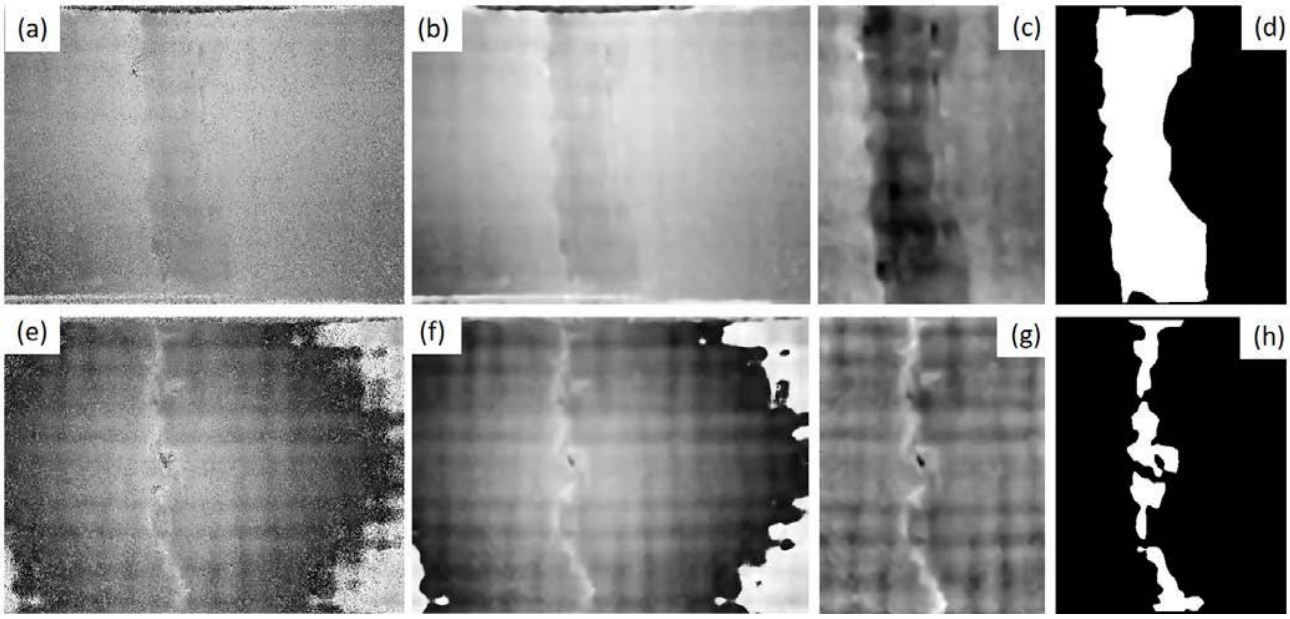

Figure 2. Example of numerical processing performed to estimate the damaged area. (a-d) The frontside of a PA6BS specimen is shown. (e-h) The backside of the same specimen is shown. (a, e) Acquired data. (b, f) Denoised data. (c, g) ROI after background calibration. (d, h) Damaged areas.

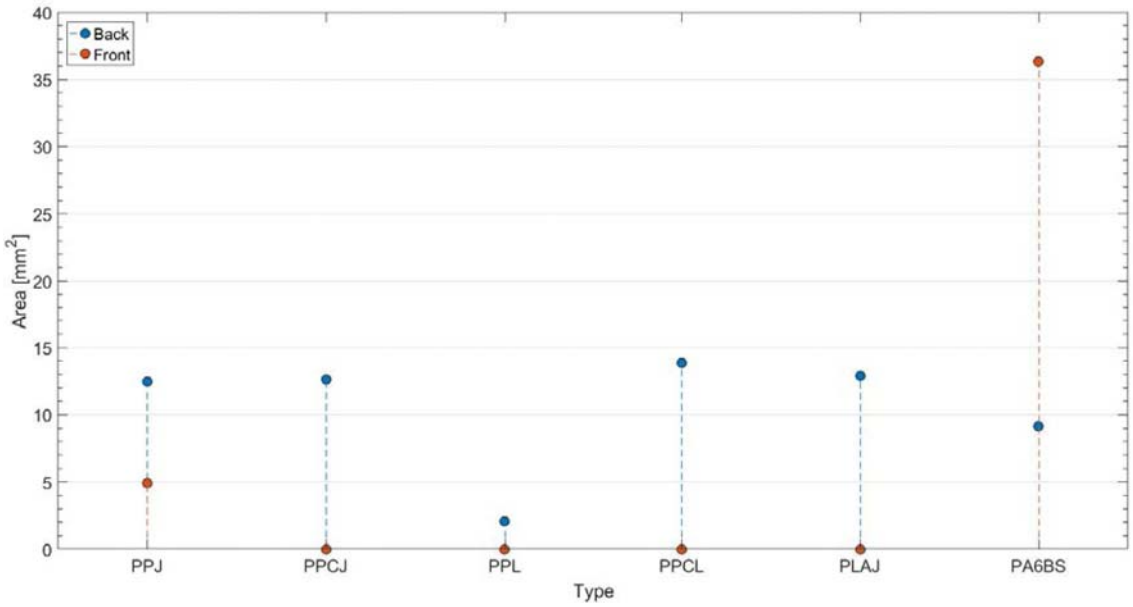

Figure 3: Damaged Area determined by ESPI.

4. Conclusions

The flexural damage of six different types of composites including woven natural fibers has been considered. In particular, the attention was focused on systems obtained by combining three thermoplastic

matrices, polypropylene (apolar resin), poly(lactic acid) and polyamide 6 (polar resins), with also the inclusion of a coupling agent in the former case, with three kind of natural reinforcing fibers as linen, jute and basalt.

The damaged areas were investigated by means of ESPI to assess their actual extent. The results show that the interfacial adhesion significantly affects damage mechanisms and, consequently, the flexural parameters of the investigated composite materials, improving their performances with the increase of the fiber-matrix affinity. Moreover, the extent of the damage takes into account, among others, of the different type of stress at which plies on both sides of each specimens, with respect of the applied flexural load, are subjected. The damage, always detected in the side subjected to tensile stresses (backside), is generally negligible on the front side, in direct contact with the bending tool, subjected to compression stresses. The exception is the PA6BS system given its relatively high flexural rigidity.

Finally, with the awareness that SEM morphological observations, highlighting different damage mechanisms occurring on front and back side of tested specimens as well as the effect of the grafting agent, may support the detected flexural and damage results and provide a significant contribution about actual potentiality of studied composite systems, tests are still in progress.

References

[1] Pickering KL, Aruan Efendy MG and Le T A review of recent developments in natural fiber composites and their mechanical performance 2016 *Comp. Part A: Appl. Sci. Manufact.* **83** 98
[2] Papa I, Lopresto V, Simeoli G, Langella A and Russo P Ultrasonic damage investigation on woven jute/poly(lactic acid) composites subjected to low-velocity impact 2017 *Comp. Part B* **115** 282
[3] De Rosa IM, Santulli C and Sarasini F Acoustic emission for monitoring the mechanical behavior of natural fiber composites: A literature review 2009 *Comp. Part A: Appl. Sci. Manufact.* **40** 1456
[4] Meola C, Boccardi S, Carlomagno GM, Simeoli G and Russo P In-line monitoring of jute fiber-reinforced polylactic acid subjected to impact loading by using infrared thermography 2017 *J. Appl. Polym. Sci.* **134** 45579
[5] Georges MP, Thizy C, Languy F and Vandenrijt JF An overview of interferometric metrology and NDT techniques and applications for the aerospace industry 2016 Proc. of SPIE **9960** 996007
[6] Pagliarulo V, Rocco A, Langella A, Riccio A, Ferraro P, Antonucci V, Ricciardi MR, Toscano C and Lopresto V Impact damage investigation on composite laminates: comparison among different NDT methods and numerical simulation 2015 *Meas. Sci. Technol.* **26** 085603
[7] Pagliarulo V, Palummo R, Rocco A, Ferraro P, Ricciardi MR and Antonucci V Evaluation of delaminated area of polymer/carbon nanotubes fiber reinforced composites after flexural tests by ESPI 2014 *IEEE MAS Proc.* **6865922** 211
[8] Antonucci V, Caputo F, Ferraro P, Langella A, Lopresto V, Pagliarulo V, Ricciardi MR, Riccio A and Toscano C Low velocity impact response of carbon fiber laminates fabricated by pulsed infusion: A review of damage investigation and semi-empirical models validation 2016 *J Progress Aerospace Sci* **81** 26
[9] Bianco V, Memmolo P, Paturzo M, Finizio A, Javidi B and Ferraro P Quasi noise-free digital holography 2016 *Light: Science & Applications* **5(9)** 16142
[10] Bianco V, Memmolo P, Paturzo M. and Ferraro P On speckle suppression in IR digital holography 2016 *Opt. Lett.* **41(22)** 5226